

Supporting Information

Spatiotemporal control of doxorubicin delivery from ‘stealth’-like prodrug micelles

Li Kong, Dimitrios Poulcharidis, Gregory F Schneider, Frederick Campbell and Alexander Kros**

Contents

Synthesis of **1**

Figure S1 – ¹H NMR of **3**

Figure S2 – ¹H NMR of Doxorubicin

Figure S3 – ¹H NMR of **1**

Figure S4 – Analytical HPLC of **1**.

Figure S5 – ESI-MS (raw) spectra following photolysis of **1**.

Figure S6 – Deconvoluted mass spectra of nitroso-PEG envelope

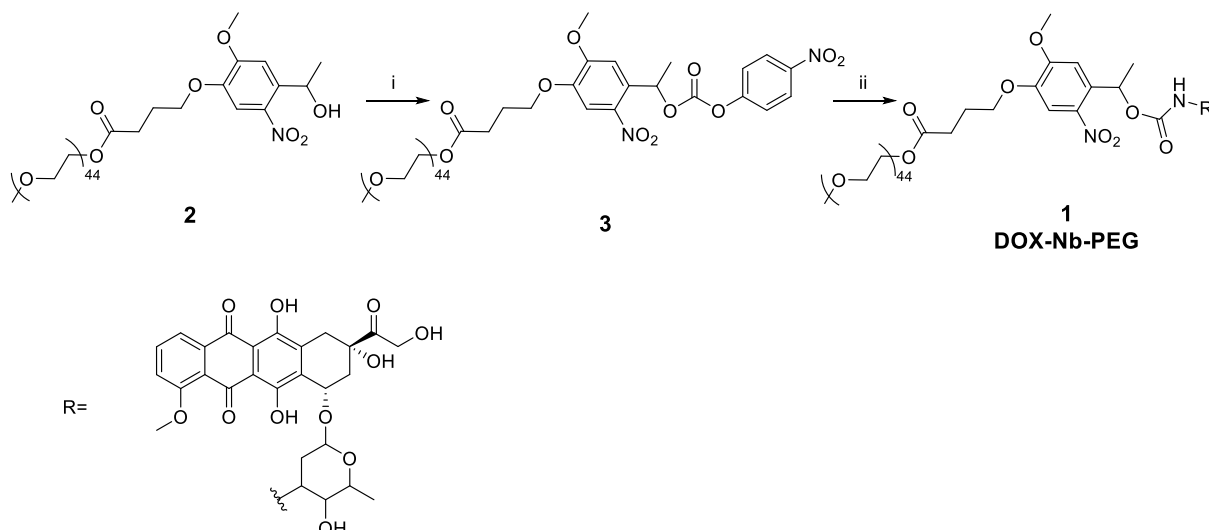
Figure S7 – DLS size distributions of **1** over time and at varying concentrations.

Figure S8 – Bright-field images of cells following varying UV irradiation time.

Figure S9 – FACS analysis of DOX uptake varying UV irradiation time

References

Synthesis of 1



Synthetic scheme to 1. (i) 4-nitrophenylchloroformate, Et₃N, CH₂Cl₂. (ii) Doxorubicin.HCl, Et₃N, DMF.

MethoxyPEG₂₀₀₀ 4-(4-(1-hydroxyethyl)-2-methoxy-5-nitrophenoxy)butanoate (2) was synthesized as previously reported ^[1].

MethoxyPEG₂₀₀₀ 4-(2-methoxy-5-nitro-4-(1-(((4-nitrophenoxy)carbonyl)oxy)ethyl)phenoxy)butanoate, 3

To a stirred solution of **2** (500 mg, 0.22 mmol) and 4-nitrophenyl chloroformate (265 mg, 1.31 mmol, 6eq.) in CH₂Cl₂ (20mL) was added Et₃N (305 μ L, 2.19 mmol, 10eq.). The reaction mixture was stirred at room temperature in the dark overnight. Following solvent removal *in vacuo*, purification by column chromatography (*Gradient*: CH₂Cl₂ to 15% MeOH in CH₂Cl₂) afforded **3** (278 mg, 0.11 mmol, 52%) as a yellow powder.

R_f: 0.30 (CH₂Cl₂:MeOH; 12:1)

¹H NMR (CDCl₃, 400 MHz): 8.26 (d, *J* = 8 Hz, ArH-*o*-NO₂, 2H); 7.61 (s, ArH-*o*-NO₂, 1H); 7.35 (d, *J* = 8 Hz, ArH-*m*-NO₂, 2H); 7.11 (s, ArH-*m*-NO₂, 1H); 6.52 (q, *J* = 8 Hz, CH(CH₃)OCOO, 1H); 4.26 (m, COOCH₂CH₂O, 2H); 4.14 (t, *J* = 8 Hz, OOCCH₂CH₂CH₂O, 2H); 4.00 (s, CH₃O, 3H); 3.45-3.95 (m, OCH₂CH₂, 196H); 3.32 (s, CH₃OCH₂CH₂O, 3H); 2.59 (m, OOCCH₂CH₂CH₂O, 2H); 2.19 (m, OOCCH₂CH₂CH₂O, 2H); 1.78 (d, *J* = 8 Hz, CH(CH₃)OCOO, 3H).

MethoxyPEG₂₀₀₀ 4-(4-(1-(((3-hydroxy-2-methyl-6-(((1S,3S)-3,5,12-trihydroxy-3-(2-hydroxyacetyl)-10-methoxy-6,11-dioxo-1,2,3,4,6,11-hexahydrotetracen-1-yl)oxy)tetrahydro-2H-pyran-4-yl)carbonyl)oxy)ethyl)-2-methoxy-5-nitrophenoxy)butanoate, 1

To a stirred solution of **3** (86 mg, 0.034 mmol) and doxorubicin.HCl (20 mg, 0.037 μ mol) in DMF (500 μ L) was added Et₃N (47.2 μ L, 0.34 mmol, 10eq.). The reaction mixture was stirred at RT in the dark overnight. CH₂Cl₂ (20 mL) was then added to the reaction mixture and the solution washed with brine (15 mL). The organic fraction was dried (Na₂SO₄) and solvent removed *in vacuo*. Column chromatography (*Gradient*: CH₂Cl₂ to 2% MeOH in CH₂Cl₂ to 10% MeOH in CH₂Cl₂) yielded **1** (58.1 mg, 61%) as a red powder.

R_f: 0.20 (CH₂Cl₂:MeOH; 12:1)

¹H NMR (CDCl₃, 400 MHz): Partial peak assignment annotated in Figure S3. ¹H NMR of DOX with partial peak assignment included in Figure S2.

MS – despite numerous attempts to characterize this compound (MALDI, ESI), MS data was inconclusive – most likely due to compound instability and/or poor ionization of this compound during mass spec analysis. Following UV irradiation however, the MS of the photolysis products could be clearly detected (Figure S5 and S6). These products – nitroso-PEG and DOX – can only arise from the photolysis of **1**.

Supporting Information Figures

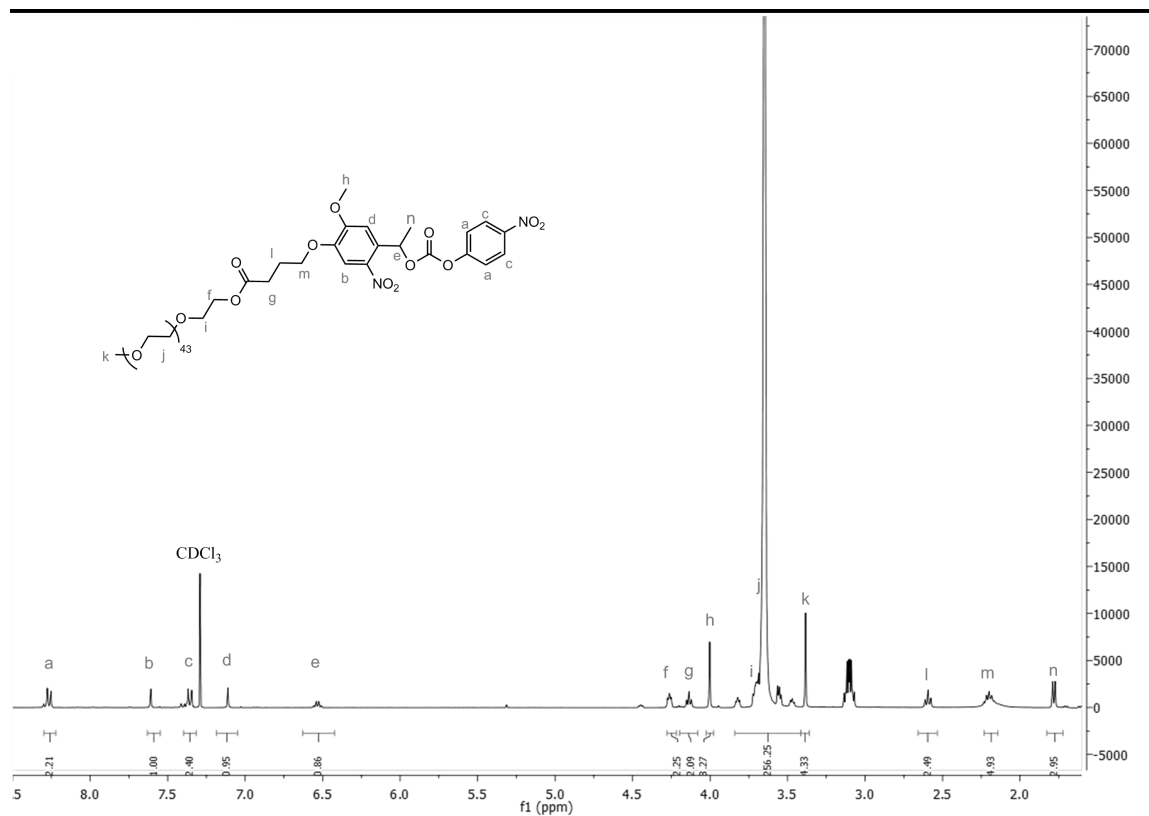


Figure S1. $^1\text{H-NMR}$ of **3**.

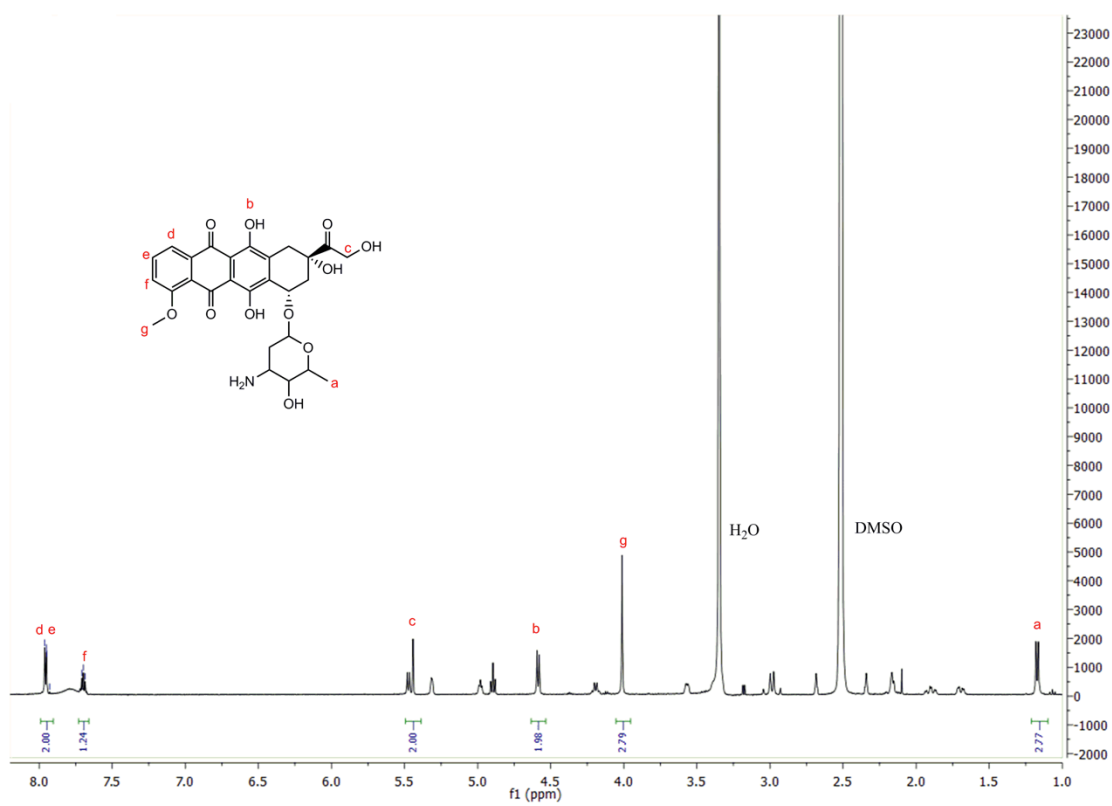


Figure S2. $^1\text{H-NMR}$ of **Doxorubicin**.

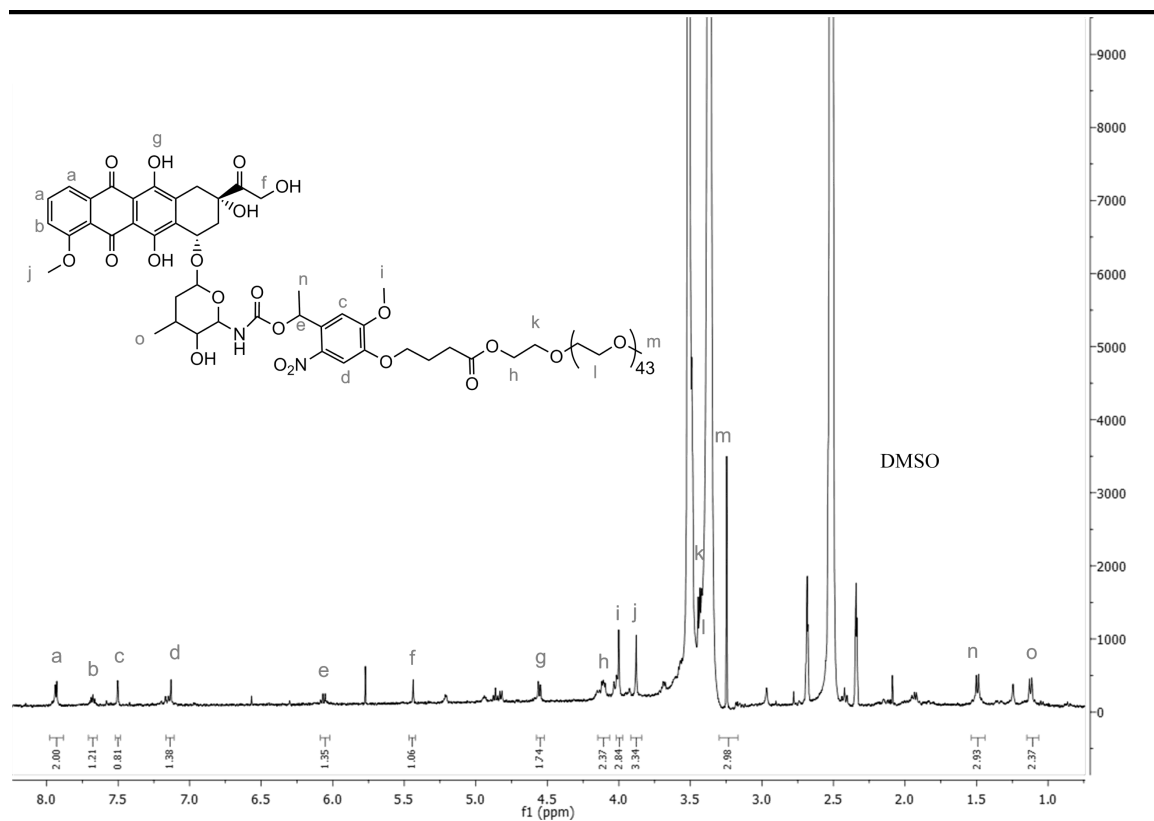


Figure S3. ¹H-NMR of **1**.

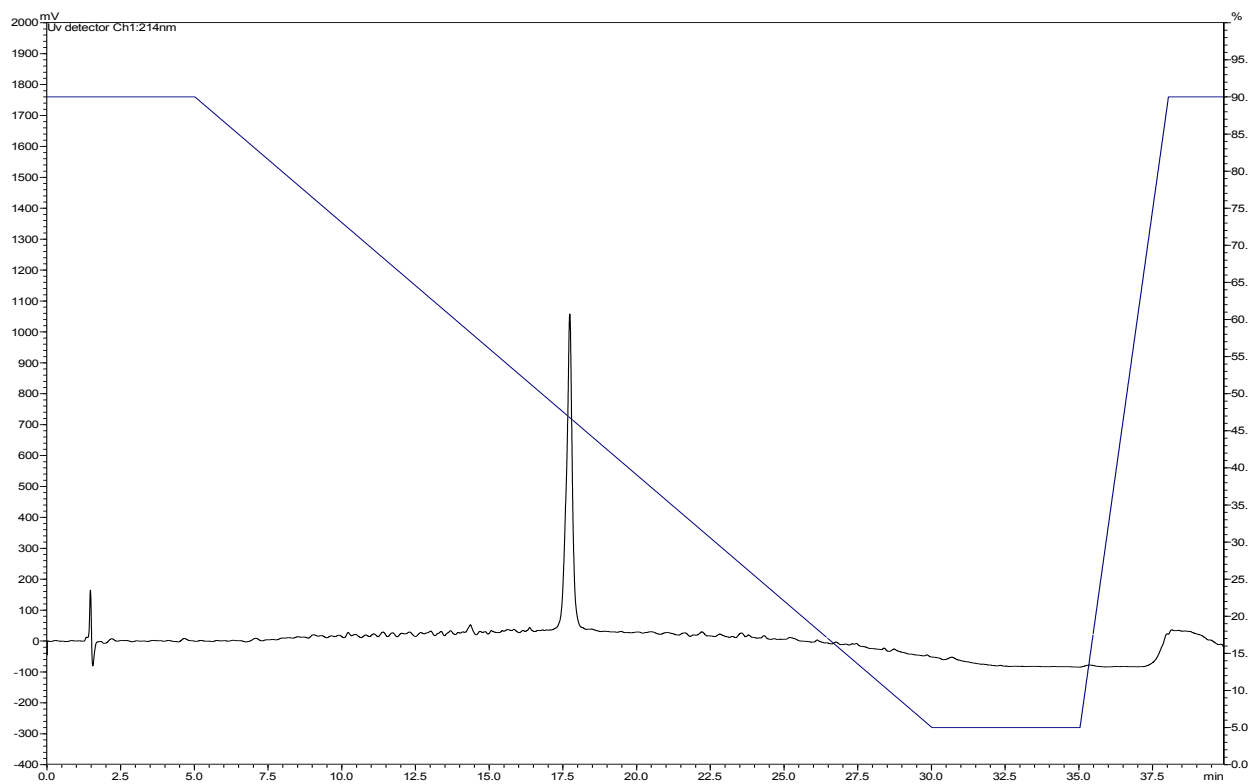


Figure S4. HPLC trace of **1**. Retention time – 17.8 min. UV detection – 214 nm.

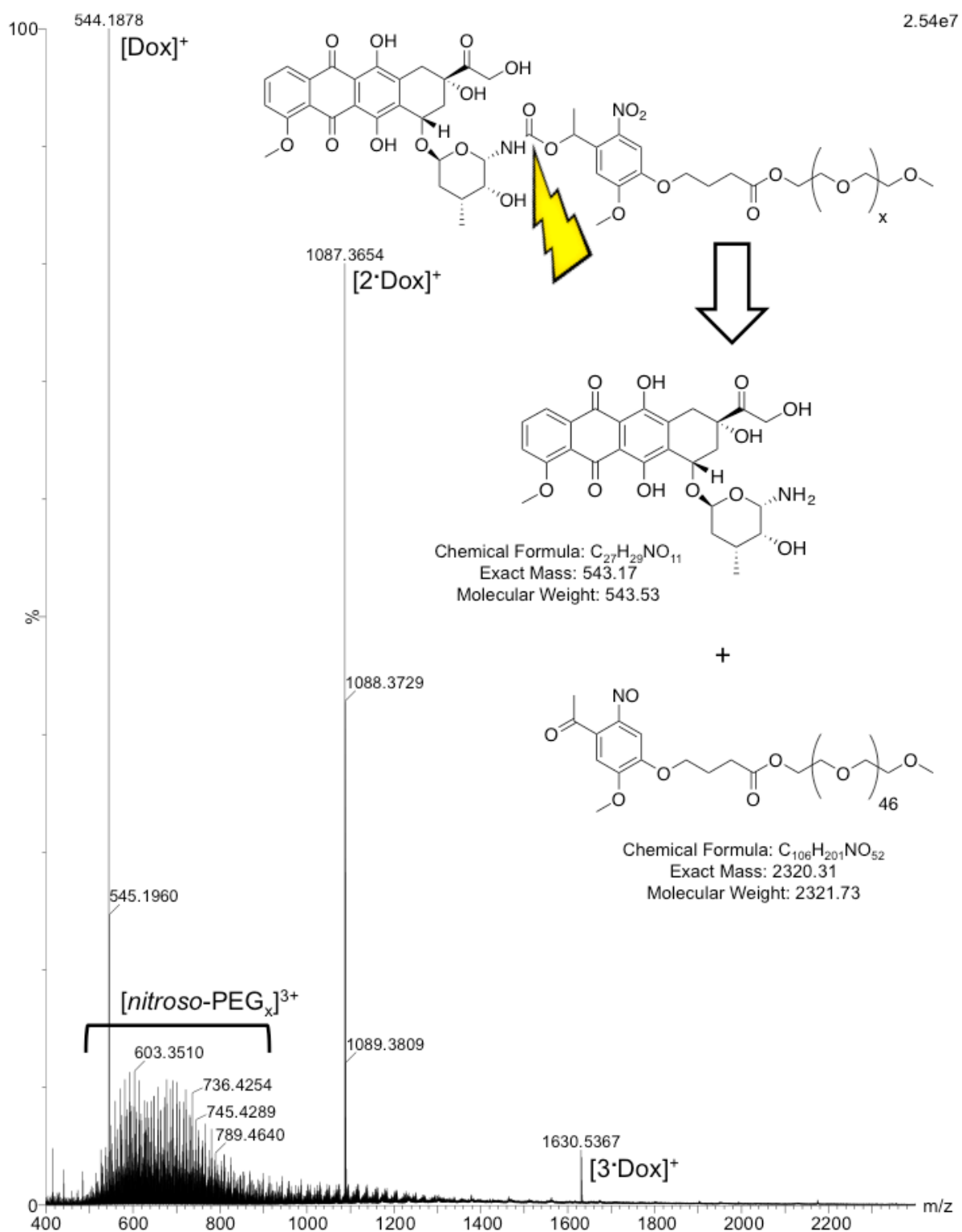


Figure S5. ESI-MS spectra (raw data) following photolysis of **1** and showing the expected photoproducts – DOX and nitroso-benzyl-PEG₂₀₀₀ – as the only significant species present. The presence of DOX clusters – [2·DOX]⁺ and [3·DOX]⁺ – in the raw spectra arise from ‘soft’ electrospray ionization techniques.

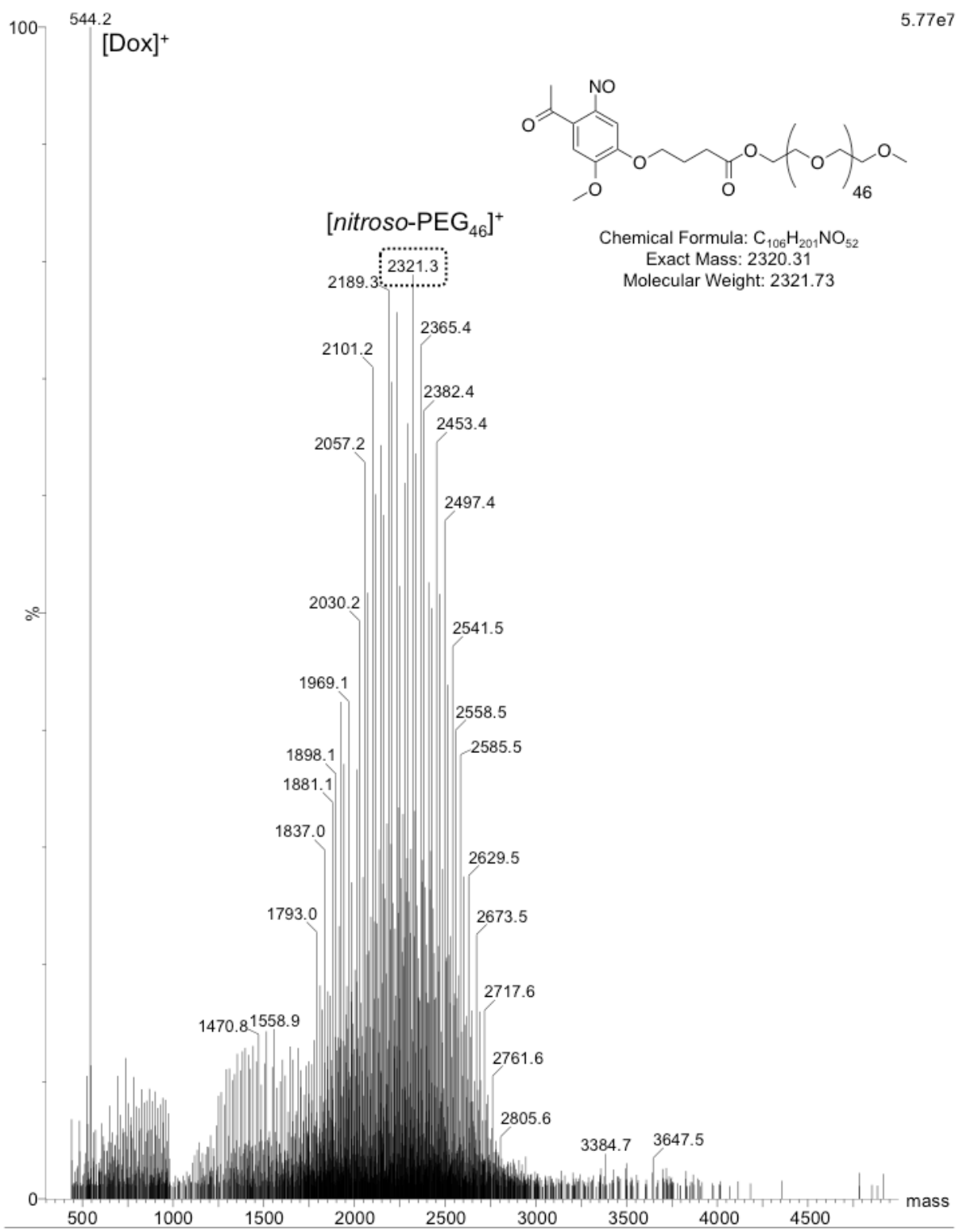


Figure S6. Deconvoluted (*software*: MaxEnt1) mass spectra of nitroso-PEG envelope signals.

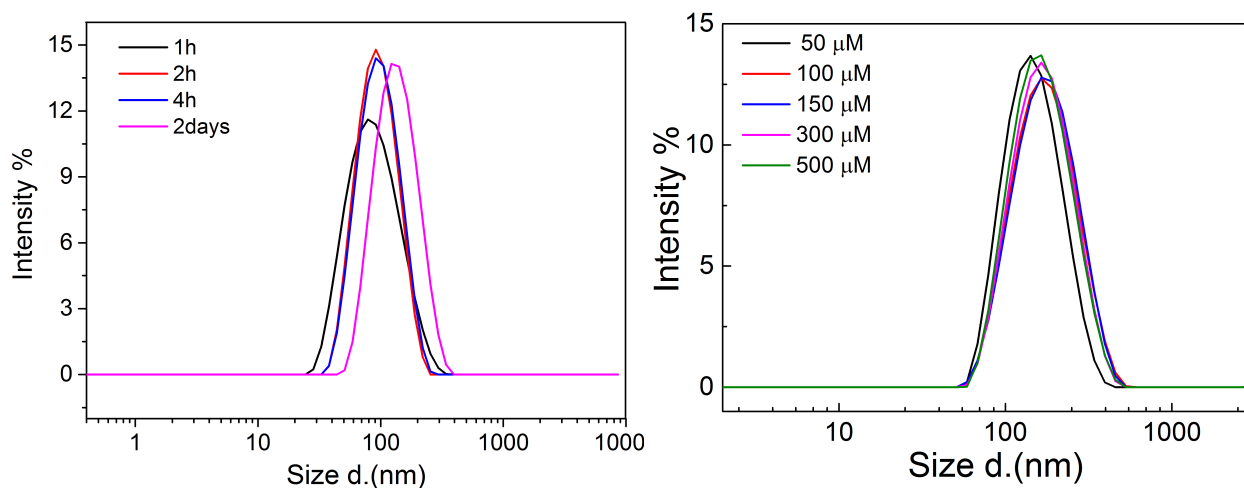


Figure S7. (left) Time course DLS size distributions of **1** (300μM in PBS) diluted (1:1) in DMEM+FCS. (right) DLS size distributions of **1** (varying concentrations) in PBS.

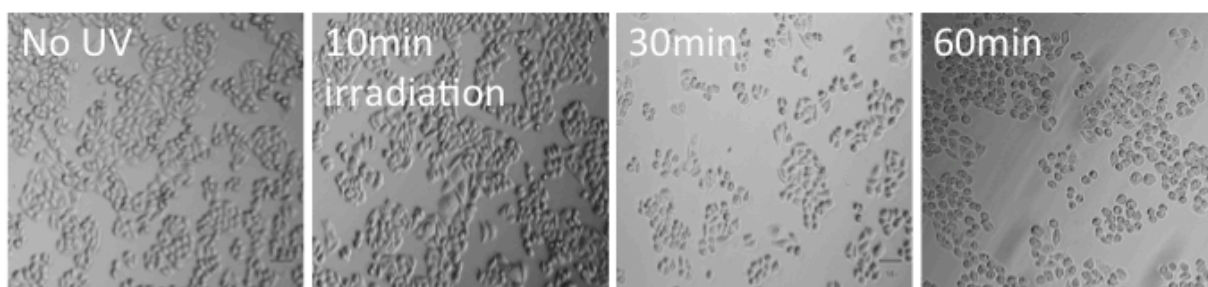


Figure S8. Cells (bright field) irradiated for varying times (UV-A, 365nm, 15-17 mWcm⁻²) and imaged immediately. As UV-A irradiation times increase cells become smaller (shrinkage) and more rounded, hallmarks of the onset of UV-A induced apoptosis.²

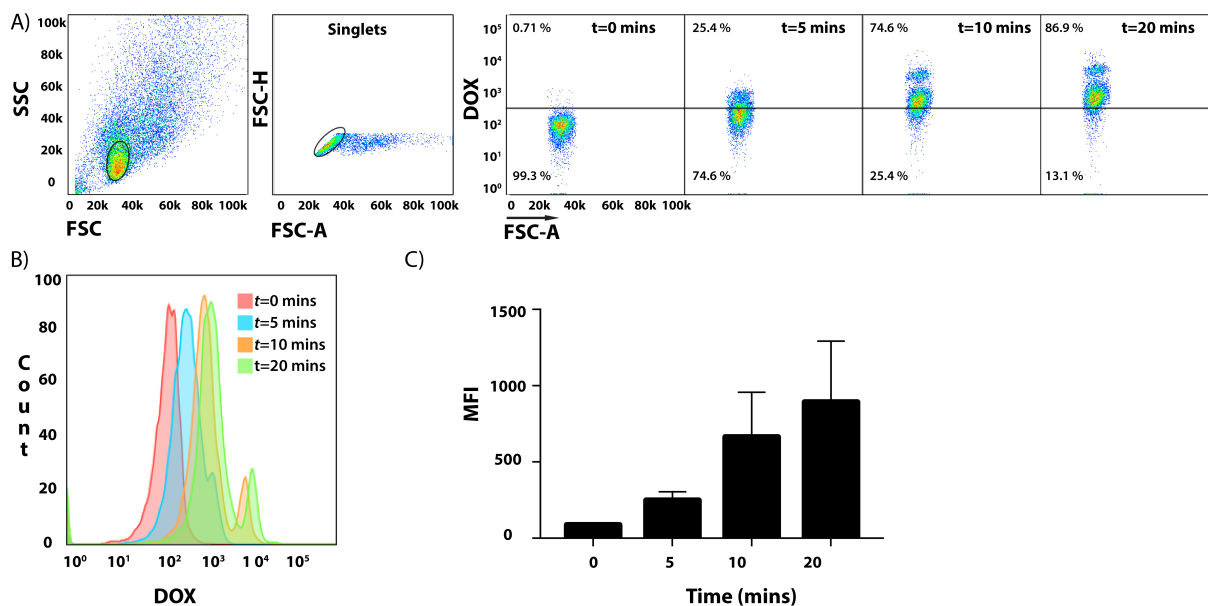


Figure S9. FACS analysis showing increased uptake of DOX (released from a solution of **1** ($300\mu\text{M}$ in PBS)) by HeLa cells with increasing irradiation times. A) Dot plots of HeLa cells after $t=0$, 5, 10 and 20 mins of irradiation; cell population was gated based on FSC-A vs SSC-A (cell doublets were gated out using FSC-A vs FSC-H). B) Histograms of HeLa cells after $t=0$ mins (pink), $t=5$ mins (blue), $t=10$ mins (orange) and $t=20$ mins (green) irradiation. C) Mean Fluorescence Intensity (MFI) of HeLa cells after different irradiation times. Error bars \pm SD.

References

- [1] Kong, L.; Askes, S. H. C.; Bonnet, S.; Kros, A.; Campbell, F. *Angew. Chem. Int. Ed.* **2016**, *55*, 1396–1400.
- [2] Elmore, S. *Toxicol. Pathol.* **2007**, *35*, 495–516.